

THERMAL SIMULATION OF NiCd BATTERIES FOR SPACECRAFT

P. MONTALENTI

*European Space Agency, European Space Technology Center, Domeinweg, Noordwijk
(The Netherlands)*

P. STANGERUP

Elektronikcentralen DK-2970 Hørsholm (Denmark)

(Received March 10, 1977)

Summary

NiCd cell and battery behaviour was studied in typical spacecraft operating conditions, both theoretically and experimentally.

The first stage of the study consisted in generating a model for the temperature distribution inside the cell for given heat generation values and confirming its validity through specific tests.

The second stage consisted in predicting heat generation inside the cell in different operating conditions and checking prediction validity through testing.

The third stage consisted in generating by network analysis a model of the thermal behaviour of a full-scale battery in actual spacecraft operating conditions. Experimental results were very close to results of the battery simulation exercise.

The battery simulation model produced can be used to predict the thermal behaviour of a NiCd battery in most of the possible spacecraft operating conditions.

Introduction

In most earth satellites the main source of power is formed by photovoltaic solar cells. In order to provide power during eclipses and peak-load demand periods, electrochemical energy storage systems are used. A NiCd sealed cell battery is the most popular energy storage system due to its high reliability and extended lifetime.

The battery is normally mounted on-board the spacecraft through feet that can either be thermally insulating or conducting to the spacecraft structure. In addition to the feet, the battery is thermally coupled to the facing parts of the satellite, namely: operative units, structure, insulating external shroud, radiators (windows or louvres), by radiation. A typical satellite disposition is shown in Fig. 1.

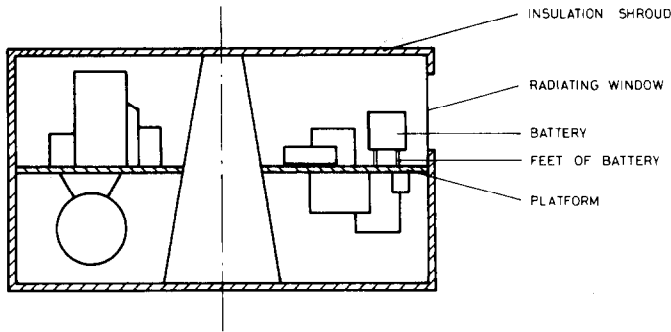


Fig. 1. Typical satellite configuration.

In order to maximize the battery's lifetime, temperature difference between cells must be kept to a minimum and the battery's temperature between preset limits. To achieve this a good knowledge of battery thermal behaviour is necessary.

The scope of this paper is to show the possibility of thermal simulation of a NiCd cell and battery through the use of simple thermodynamic relations and computer simulation of an equivalent electric network.

Temperature distribution found by finite difference method

When the heat evolution within the NiCd cell is known, it is of great importance to be able to determine the temperature distribution in the cell as a result of its internal structure.

If all the thermal properties of the cell materials are known, the temperature distribution can be determined for any thermal load conditions. As will be shown, this can easily be done by means of computer programs using the finite difference method. The greatest problem will probably be that of obtaining an adequate thermal model of the cell. However, experience has shown that even quite coarse models yield reasonable results in the computation [1].

The solution of many temperature distribution problems is that of the Poisson equation:

$$\Delta v = -\frac{Q}{K}$$

where v is excess temperature, Q is heat generation per unit volume and time, and K is the thermal conductivity. It is well known that the Poisson equation can be solved analytically only in a few and very special cases. Therefore, numerical methods are normally used. In the finite difference method the Poisson equation is replaced by a set of linear equations assumed to characterize the problem adequately.

These finite difference equations are achieved by a Taylor series expansion. This corresponds to breaking a three-dimensional body up into sub-volumes each representing a node in a network. The conductances connecting these nodes are determined by the conductivity and the fineness of the division.

Thus, the solution of the problem has been turned into that of solving a large number of linear equations.

Computer-aided solution of a large number of linear equations

Even a relatively coarse division of a three-dimensional body into sub-volumes will produce networks with several hundred nodes, *i.e.* equations.

The conductance matrix is normally, and especially for finite difference systems, very sparsely filled with non-zero elements. This is due to the fact that each node is only connected to its 6 adjacent nodes. In practice, solution methods exploit this feature. The successive over-relaxation (*SOR* method) is a very simple iterative process to use with a computer, having the advantage of a very small storage demand. However, because of the many convenient routines developed in connection with computer programs for electrical networks, these can be recommended if the number of nodes can be kept smaller than some few hundred. These programs making use of direct solution techniques, such as the Gauss elimination, contain sparse matrix routines as well as very efficient sensitivity routines. Furthermore, the direct solution technique is more convenient in connection with time-varying problems.

The NiCd cell has been analyzed using already existing network programs with minor modifications and converting thermal units into electrical equivalents. The sensitivity routine yielding the variation of the excess temperatures as a result of a change in the thermal properties of materials, has been shown to be a very efficient means of finding critical points in thermal designs.

Thermal analysis of NiCd cells

Figure 2 shows the structure of a typical prismatic NiCd cell. For the thermal analysis, the cell can be divided into two major parts: (a) an inner block consisting of the positive and negative electrodes and the separator; (b) a stainless-steel case containing the block. The two parts are separated by a thin sheet of insulating material. Most of the thermal data for materials used in NiCd cells are taken from the work of Brooman and McCallum [2].

The thermal properties for the inner block are different in directions parallel to the plates and perpendicular to the plates. Perpendicular to the plates the conductivity is determined by a series connection of the conductances through positive and negative plates as well as through the separators. The conductivity through the plates in this direction is somewhat difficult to predict and may vary considerably, especially with the state of charge of the cell. An average value of $0.5 \text{ W/}^\circ\text{C/m}$ is used in the calculations.

The conductivity in the direction parallel to the plates is found from a parallel connection of the conductances. The above considerations lead to the following conductivities for use in the analysis:

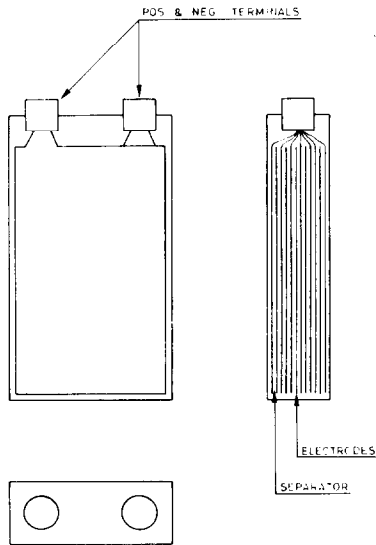


Fig. 2. Typical NiCd cell.

Inner block:

parallel to plate: $K_{\parallel} = 10.2 \text{ W/}^{\circ}\text{C/m}$

perpendicular to plate: $K_{\perp} = 0.36 \text{ W/}^{\circ}\text{C/m}$

Case (stainless steel): $K_{\text{case}} = 12.5 \text{ W/}^{\circ}\text{C/m}$

The thermal conductance of the medium between the inner block and case is difficult to predict. A thin sheet of insulating material separates the block from the case but, due to mechanical inaccuracies, areas of small gas gaps must be considered as part of this medium. The following average values have been chosen for the separating medium:

Thickness (mm)	Specific conductance (W/ $^{\circ}\text{C/m}$)
XZ 0.15	0.1
YZ 0.5	0.05
XY 1.0	0.05

The thicknesses have been evaluated from X-ray photographs. XZ denotes the large side of the cell. The tightest thermal connection between block and case is assumed to take place there.

Steady state analysis of NiCd cells

Figure 3 outlines an experiment that in a simple way could verify the thermal model. The cell was placed in an aluminium box with four well-defined thermal contacts to the ambient. Heat dissipation by radiation was avoided by insulating with Rockwool.

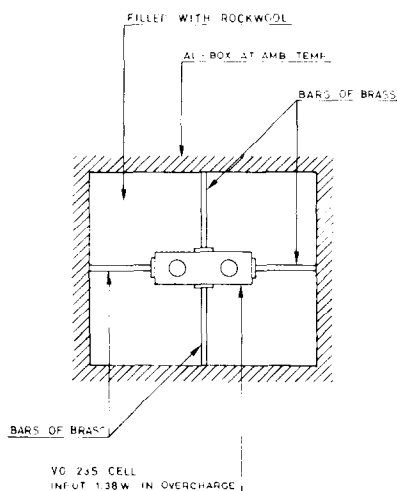


Fig. 3. Experimental verification of thermal model for a NiCd cell.

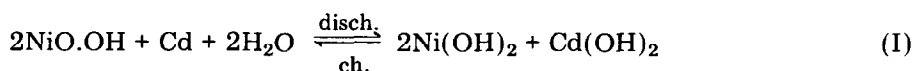
Temperatures were measured at various points of the surface of the cell. The input power was 1.38 W in the over-charge mode, *i.e.* all the power is assumed to produce heat.

The results of this experiment are shown in Fig. 4. It is seen that the agreement between measured and calculated temperatures is quite good. It is difficult to determine the exact values of conductances around the terminals and the greatest discrepancy is found here. On the other hand, sensitivity calculations show that the values of the thermal properties for the medium separating the block and the case can be chosen within quite large ranges without affecting the temperature distribution very much, even for quite heavy thermal loading of the cell.

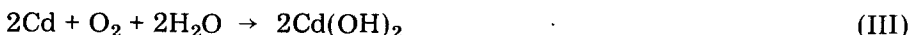
Thermal model of NiCd cells

Cell reactions

The main overall reaction in a NiCd cell is:



When operating with correctly manufactured NiCd cells, one reaction only occurs during discharge. During charge and overcharge, oxygen is evolved on the nickel electrode and chemically recombined on the cadmium electrode following the scheme of reactions (IIa) and (III).



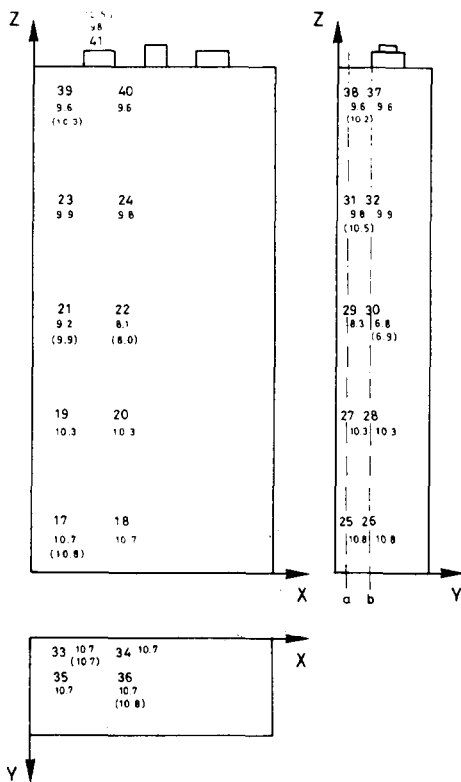


Fig. 4. Result of experiment shown in Fig. 3. Temperatures indicated below node numbers are computed and measured (in parentheses).

As a consequence the charge efficiency is always lower than 1. Hydrogen evolution on the negative electrode is avoided in sealed elements by providing an excess of reduced negative capacity during manufacture.

A certain amount of the evolved oxygen is accumulated in the free volume of the cell during charge and overcharge. This amount is dependent on the charge rate, the free volume inside the cell and inversely on the rate of reaction (III). The last factor is difficult to determine and can vary strongly from cell to cell. In the following development of a thermodynamic model of the cell the effect of the accumulated oxygen will be, for simplicity, neglected and heat and electricity will be the only forms of energy considered in connection with cell operation, together with the chemical energy connected with the principal reaction.

Enthalpy of the main reaction

The following values are used for the calculation of the enthalpy of reaction:

$$\text{Ni(OH)}_3 \Delta H = -162.1 \text{ kcal} \quad (3)$$



The resulting enthalpy for reaction (I) is $\Delta H_T = -66.2 \text{ kcal}$.

Heat evolution equations

The free energy of a chemical reaction or "Gibbs potential of reaction" is:

$$\overline{\Delta G} = \overline{\Delta H} + T \overline{\Delta S}$$

and is the amount of energy ideally convertible into electricity when only one electrochemical mechanism is involved. $T \overline{\Delta S}$ is the amount of energy evolved as heat, and $\overline{\Delta H}$ is the enthalpy of the reaction. The standard (equilibrium at 25 °C) potential of an electrochemical reaction is given by:

$$E_0 = K \frac{\overline{\Delta G}}{zF} = \frac{K}{zF} (\overline{\Delta H} + T \overline{\Delta S})$$

where $K = 4.184 \text{ joules/kcal}$, z is the number of electrons exchanged in the reaction, $F = 96,500 \text{ A s/gequiv}$. (Faraday constant).

The power converted into electricity in ideal operation is:

$$W_i = K \frac{\overline{\Delta G}}{zF} \cdot i$$

the power dissipated:

$$Q_i = K \frac{T \overline{\Delta S}_i}{zF} = \frac{K}{zF} (\overline{\Delta H} - \overline{\Delta G}) i$$

In actual operation, more power is dissipated as heat as a consequence of ohmic and polarization losses:

$$Q_\Omega = (E_0 - V) i = \left(\frac{K}{zF} \overline{\Delta G} - V \right) i$$

where V = actual value of cell potential. The total power dissipated as heat during discharge of a NiCd cell is given by:

$$Q_t = Q_i + Q_\Omega = \frac{K}{zF} (\overline{\Delta H} - \overline{\Delta G}) i + \left(\frac{K}{zF} \overline{\Delta G} - V \right) i = (1.435 - V) i \quad (IV)$$

During charge, considering that all the power not converted into chemical energy following reaction (I) is converted into heat, the total amount of heat dissipated is:

$$Q_T = (Q_i + Q_\Omega) \eta + (1 - \eta) Vi = \frac{K}{zF} (\overline{\Delta H} - \overline{\Delta G}) i \eta + \left(\frac{K}{zF} \overline{\Delta G} - V \right) i \eta + Vi(1 - \eta) = i [(V - 1.435) \eta + V(1 - \eta)] \quad (V)$$

the term $V_i(1 - \eta)$ defines the energy dissipated by the oxygen cycle of reactions (IIa), (IIb) and (III).

Equations (IV) and (V) define the heat generated during cell operation at any stage. The application needs the knowledge of η and V during operation. The efficiency diagrams and charge/discharge cell voltage diagrams relevant to the practical case analyzed, as well as a procedure for their use, are given here below.

Charge efficiency*

Charge efficiency of European NiCd space elements is known for a wide range of charge rates and temperatures covering all foreseen spacecraft operating conditions. Figure 5 is a typical example of instantaneous charge efficiency diagram [5]. In such diagrams, the instantaneous efficiency is given as a function of the charged capacity. The charged capacity C_c is the capacity delivered to the cell from an external source at a given rate after the cell has been discharged with a $C/2$ rate to a potential of 1 V. The discharged capacity C_d is the capacity delivered by the cell when discharged at $C/2$ to 1 V.

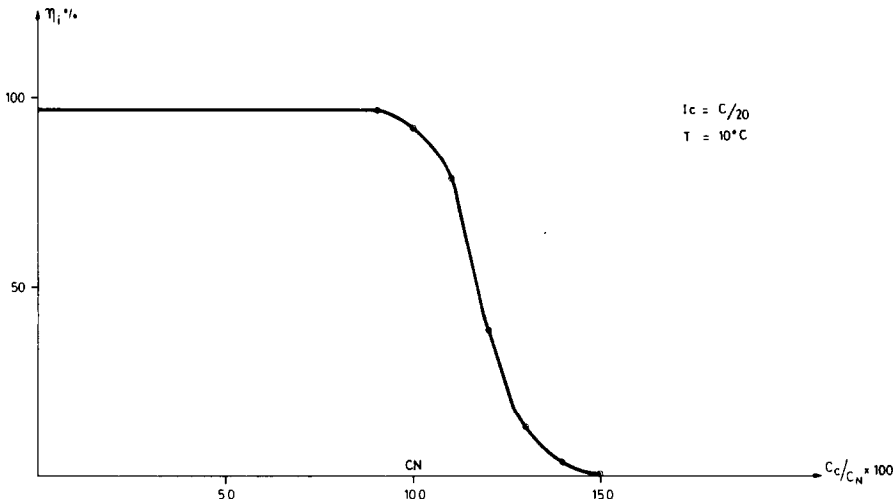


Fig. 5. Instantaneous charge efficiency of SAFT NiCd cells. C_c = charged capacity; C_N = nominal capacity.

Figure 6 shows the C_d versus C_c diagram from which the instantaneous efficiency diagram was derived. Figure 7 shows a simplified efficiency diagram used for the calculations reported below.

Part of the charged capacity is accumulated into the cell through the principal electrochemical reaction, part of it is utilized by unwanted side reactions.

*By charge efficiency we intend instantaneous amperhour charge efficiency which is "the ratio between discharged and charged capacity over a cycle whose amplitude tends to zero".

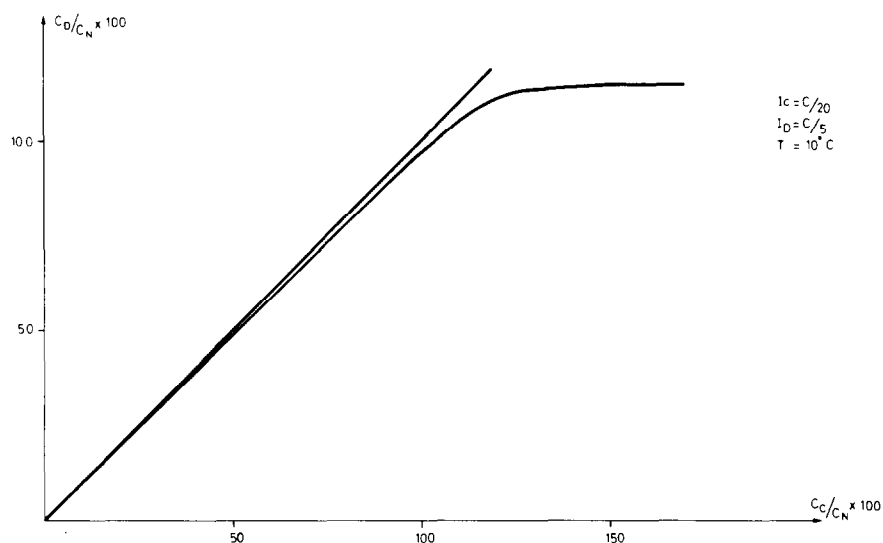


Fig. 6. C_d versus C_c diagram for SAFT NiCd cells.

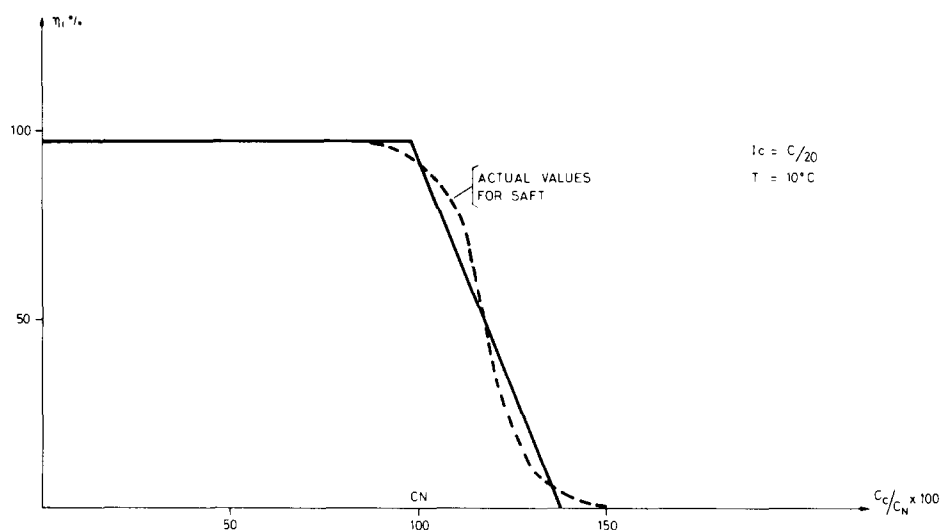


Fig. 7. Simplified instantaneous efficiency diagram.

The instantaneous efficiency is the ratio between the rate of the usefully accumulating capacity C_{cu} and the given rate of charge:

$$\eta_i = \frac{dC_{cu}}{dt} \cdot \frac{1}{i}$$

The use of the efficiency diagrams to predict heat evolution from the cell is somewhat troublesome since the knowledge of the "state of charge", necessary for the use in the instantaneous efficiency diagrams, is not achievable

with accuracy through normal monitoring of cell operation conditions.

A correct use of the efficiency diagrams is possible in the case of cycling with a fixed charge factor $K = C_c/C_d$ and a fixed value of discharged capacity C_d at each cycle.

Since the discharge efficiency is considered equal to 1 for any charge state and there is no change in state of charge at the beginning and end of charge from one cycle to another.

$$C_d = \int_{C_{c1}}^{C_{c2}} dC_{cu} = \int_{C_{c1}}^{C_{c2}} \eta \cdot i \cdot dt = \int_{C_{c1}}^{C_{c2}} \eta \cdot dC$$

where C_{c1} and C_{c2} are the states of charge at beginning and end of charge respectively.

The equation system:

$$C_d = \int_{C_{c1}}^{C_{c2}} \eta \cdot dC$$

$$\frac{C_{c2} - C_{c1}}{C_d} = K$$

is sufficient to locate C_{c1} and C_{c2} on the instantaneous efficiency diagram through graphical or numerical integration methods and therefore to determine the values of η to be used in the heat evolution equation during charge.

A practical method to identify C_{c1} and C_{c2} on the C_c versus C_d diagram, illustrated in Fig. 8, consists of: (a) ideally drawing a triangle with one side parallel to the C_d axis, with a length corresponding to the depth of discharge (capacity discharged at each cycle referred to the total capacity of the cell)

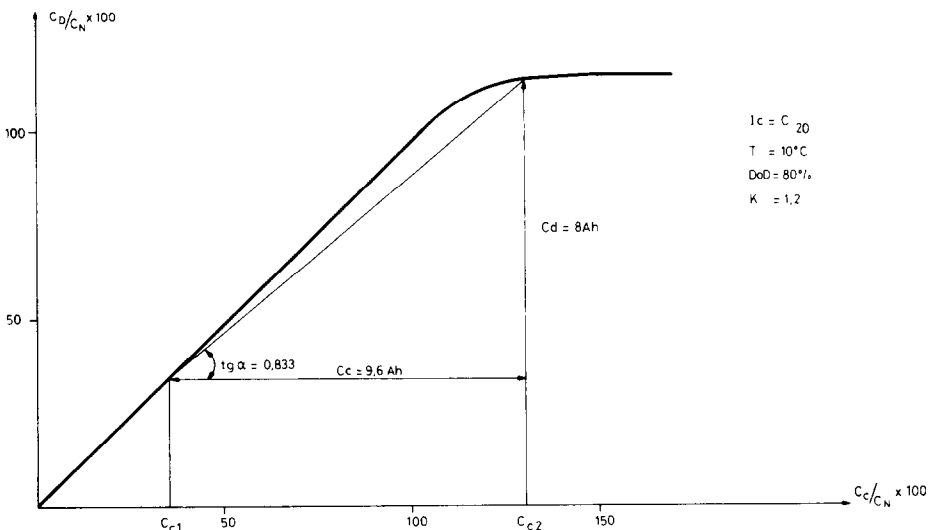


Fig. 8. Identification of initial and final state of charge.

and one side, parallel to the C_c axis, with a length of d.o.c. $\times K$; (b) shifting the triangle, keeping the cathets parallel to the axis of the diagram until the corners opposite to the rectangular angle lie on two points of the C_d versus C_c diagram.

Charge/discharge characteristics

Diagrams giving the variation of V with charge and discharge time are available from the literature in a wide range of operating conditions and can easily be experimentally traced. Figure 9 shows the charge/discharge characteristics of NiCd cells in the electrical condition relevant to the case reported here. (Cycling with 80% depth of discharge, a charge rate of $C/20$, a charge factor of 1.2, a discharge rate of $2C/3$ and a temperature of 10°C .)

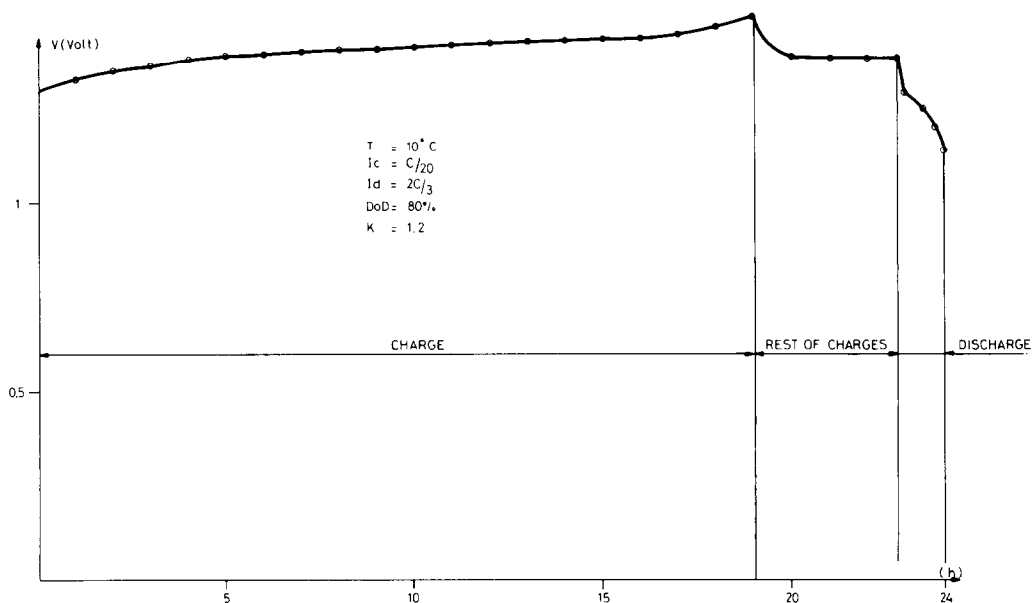


Fig. 9. Voltage evolution over a geostationary cycle.

Calorimeter measurement and simulation by computer of cell thermal behaviour

The heat flow from a cell can be measured by means of a calorimeter. During such an experiment the surface of the cell is considered isothermal because of the very efficient heat removal through the oil of the calorimeter.

If we want to simulate this by computer we interconnect all the surface nodes and load this common node with a high conductance. If, in the equivalent electrical network, this conductance is 1000 mho (much greater than conductances within the cell) the voltage in mV across this conductance will be equal to the heat flow in W from the cell.

By attaching to each node capacitors corresponding to the heat capacity of each sub-volume, the transient response corresponding to such an experiment can be found for all kinds of time-varying working modes (the time constant of the calorimeter is considered small compared to that of the cell). At the same time the node voltages indicate the time-varying excess temperatures of the inner part of the cell for efficient removal of heat from the surface.

Since the cell is to be used as part of a battery for a geostationary satellite, a simulation of a geostationary orbit cycle has been carried out. The internal heat generation and dissipation calculated using the thermodynamic relations and the calorimeter results are shown in Fig. 10.

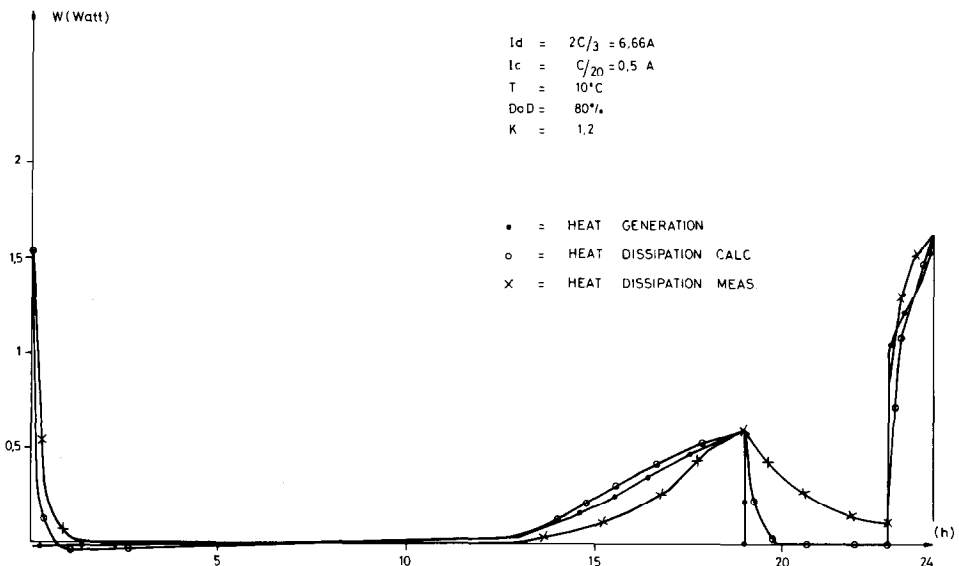


Fig. 10. Results of the heat generation calculations and heat dissipation calculations and measurements.

A reasonably good agreement is seen between measured and calculated results. Apparently the heat flow rate at the end of the charge and discharge period decreases more slowly than could be explained by the time constant.

This is deemed to be due to exothermal recombination of oxygen accumulated in the free volume inside the cell and homogenization of electrolyte concentrations.

NiCd battery for space use

Based on the experience gained by thermal analysis of NiCd cells, a battery consisting of 10 cells has been designed.

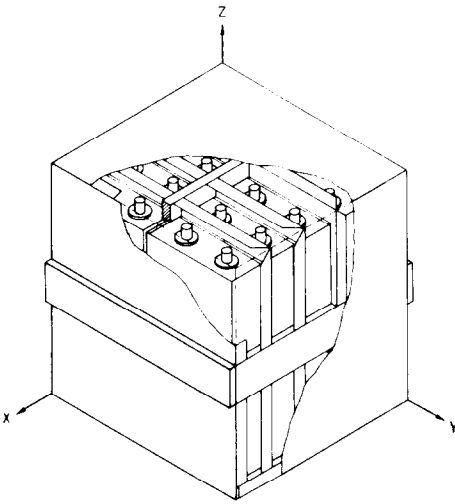


Fig. 11. Analyzed NiCd battery.

Figure 11 shows the battery. The cells are sandwiched between aluminium plates. The purpose of these plates is to drain the heat from the cells to the outer structure, which has been painted to assure a proper heat dissipation by radiation. The goal of the battery design has been to combine a lightweight structure with efficient heat removal. Furthermore, for proper operation it is important that the temperature differences between the cells within the battery are small.

For thermal analysis the battery has been broken up into a 300 node electrical equivalent network. A part of this network is shown in Fig. 12. As seen, each cell has been divided into 6 nodes. This rather coarse division is justified by the results obtained. When designing the battery a steady state thermal analysis is carried out for different thicknesses of the aluminium plates. The thinnest plates satisfying the requirements concerning excess temperatures and temperature differences within and between the cells are used in the construction.

The results of a typical network analysis are shown in Fig. 13. Radiation from the battery structure to the cold and warm side of the satellite (-40°C and 10°C respectively) has been taken into account by properly chosen "radiation resistances" in series with "temperature generators".

The analysis showed that for a total steady state internal heat generation of 10 W the temperature difference between any part of all the cells would not exceed 1°C . The temperature would be of the order of $+15^{\circ}\text{C}$. These results have been verified in practice by careful experiments and measurements.

A transient analysis simulating a certain geostationary cycle of the satellite is shown in Fig. 14. The heat generation for this charge/discharge cycle is determined by the thermoelectric processes within the cells as described previously. Heat is removed by radiation to the two sides of the satellite

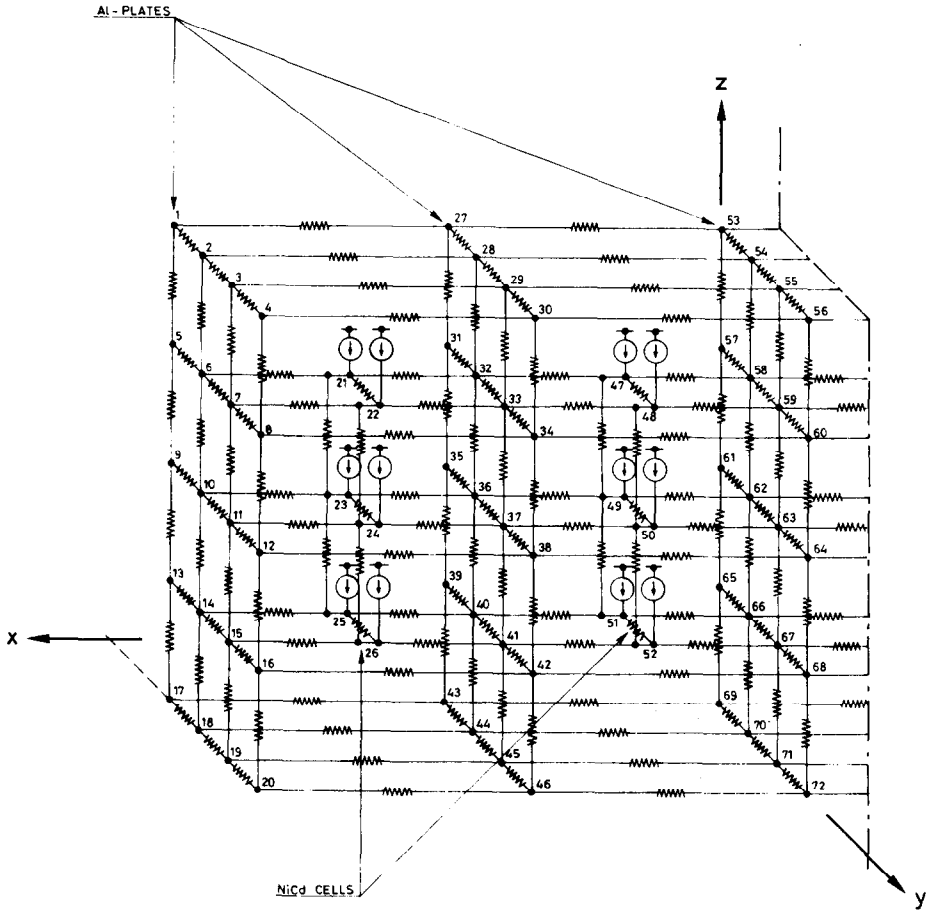


Fig. 12. Part of 300 node network corresponding to NiCd battery.

(-19°C and $+24^{\circ}\text{C}$). The small temperature gradients within the battery found by network analysis are confirmed by the measurements. All temperatures on the surface of and inside the battery are located within the shaded area. On the same diagram are shown the average values achieved by the network simulation.

The difference between the beginning and end of cycle temperatures shows the inaccuracy of the experimental results, and the error involved in the calculation.

The difference in temperature at end of charge and during open circuit between the experimental and calculated curves is due to the neglected effect of oxygen accumulation in the free volume; effect was already pointed out in this section.

In general the results shown in Fig. 14 confirm that the model elaborated can be used both for space battery design and for predicting battery behaviour.

NODE TEMPERATURES FOR BATTERY MODEL

T1=10 DEG C T2=-40 DEG C PC=10 W

STEADY STATE

NODE NO.	TEMP. DEG. C
1	13.66
2	13.71
3	13.71
4	13.60
5	13.85
6	13.88
7	13.87
8	13.82
9	13.95
10	13.97
11	13.95
12	13.90
13	13.96
14	14.00
15	13.98
16	13.91
17	13.80
18	13.82
19	13.80
20	13.72
21	15.98
22	15.98
23	16.02
24	16.02
25	16.06
26	16.05
27	13.60
28	13.66
29	13.65
30	13.60

} CELL 1

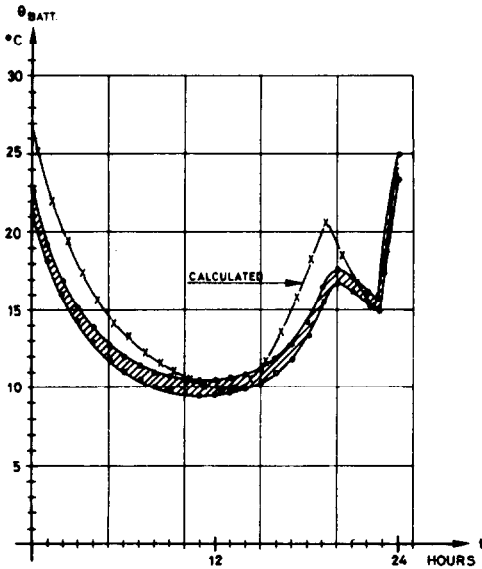
Fig. 13. Typical computer output for steady state heat evolution. Node numbers correspond to Fig. 12.

Conclusion

The test results presented in this paper show that, by using the rough simplification of cell thermodynamics and the coarse network model proposed by the authors, the thermal behaviour of a nickel cadmium battery can be predicted with a good accuracy for any possible spacecraft operating condition.

Conversely the battery thermal model can be used to define the structure and the thermal coating needed to obtain any battery temperature chosen between the temperatures of the warm and cold spacecraft units to which the battery is coupled through radiation and/or conduction.

A similar thermal network model, combined with the relevant thermodynamic model, can be used to predict the thermal behaviour of other types of batteries. Thermal battery simulation has been successfully used for the first time in Europe for the design of the silver cadmium battery of the ISEE-B spacecraft.



Test No. 18
 Test Configuration:

Battery: EC
 Test Conditions:

$$I_{CH} = C/20 = 1,15A$$

$$I_{TR.CH} = -$$

$$I_{DISCH.} = 2C/3 = 15.33A$$

$$\theta_2 = -19 \pm 1^{\circ}C$$

$$\theta_1 = +24 \pm 1^{\circ}C$$

$$p \leq 1.3 \cdot 10^{-2} \text{ N/m}^2 \text{ (} 10^{-4} \text{ Torr)}$$

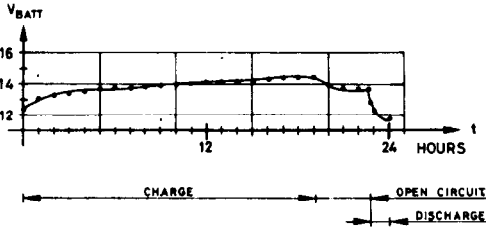
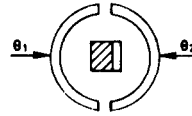


Fig. 14. Temperature of NiCd battery during geostationary cycle. All measured temperatures are within shaded area.

Acknowledgement

The authors wish to thank Mr. J. P. Bouchez for his generous collaboration in establishing the thermal model.

References

- 1 P. Stangerup, Computer aided thermal design, EC-Report ECR-56, Nov. 1975 (available from Elektronikcentralen).
- 2 E. W. Brooman and J. McCallum, The thermal conductivity of sealed nickel cadmium cells, N 72-23061, Battelle Columbus Laboratories, 1971.
- 3 Handbook of Chemistry and Physics, 45th edn., The Chemical Rubber Co., 1964-1965.
- 4 W. G. Latimer, Oxidation Potentials, 2nd edn.
- 5 P. Montalenti, Charge efficiency of sealed NiCd cells, ESA TN 136, European Space Agency, January 1977.